6378 *Inorg. Chem.* **2010**, *49*, 6378–6380
DOI: 10.1021/ic100522f

Inorganic Chemistry
Communication

Potential Hydrogen Bottleneck in Nickel−Iron Hydrogenase

Jason M. Keith and Michael B. Hall*

Department of Chemistry, Texas A&M University, College Station, Texas 77843

Received March 18, 2010

The role of two-state reactivity at the enzyme active site with respect to binding of molecular H_2 for the high- and low-spin of [NiFe] hydrogenase (Ni−SI forms) is examined by density functional theory. In addition to examination of a single H_2 molecule binding at either the Ni or Fe of the active site, the possibility that H_2 binds simultaneously at each metal center in the active site of this enzyme is examined. The concurrent binding of two molecules of H_2 suggests a potential hydrogen bottleneck in which high concentrations might lead to a decrease in the rate of hydrogen oxidation.

Currently, alternative energy has become a major issue for both economic and climatologic reasons. Of the various alternatives to fossil fuels, the one possibility most discussed is the use of molecular H_2. In an effort to further understand the design and implementation issues involved in the utilization of hydrogen, much research has been devoted to understanding how nature catalyzes the reversible oxidation of molecular H_2 ($H_2 \rightleftharpoons 2H^+ + 2e^-$) in enzymes known as hydrogenases. Three main classes of these hydrogenases have been identified and are classified based on the makeup of the transition-metal-containing active site: [NiFe] hydrogenases;[1,2] [FeFe], diiron, or Fe-only hydrogenases;[3] and monoiron or Fe−S-cluster-free hydrogenases[4] (previously mislabeled as metal-free). Diiron hydrogenases are primarily employed for proton reduction, while [NiFe] hydrogenases (the focus of this study) are employed in hydrogen oxidation.

The active site in [NiFe] hydrogenase (Figure 1) consists of an Fe atom and a Ni atom connected through two bridging cysteine ligands. The Fe atom is further complexed with two CN and one CO arranged in a square-pyramidal geometry with the CO in the axial position resulting in what is formally Fe^{II}. The Ni atom, formally Ni^{II} in the reduced electron paramagnetic resonance (EPR)-silent form (see the Supporting Information), has two additional cysteine ligands bound terminally in a seesaw or distorted tetrahedral geometry, with three of the cysteine ligands lying almost coplanar and one of the terminal cysteines bent significantly away from what would be the square plane. The resulting charge of the active site is 2− in its unprotonated form. The enzyme can exist without a bridging ligand or with a variety of bridging ligands.[2,5]

Despite the copious number of experimental and computational studies of [NiFe] hydrogenase, several questions still remain about the active site.[6] Two of the most obvious questions are: the spin state of the Ni^{II} center in the EPR-silent forms, Ni−SI (Figure 2, species **1**), singlet[7] or triplet,[8] and the H_2 binding site for activation, to the Fe, **2**, or to the Ni, **3**. Part of the confusion as to the Ni spin state is that the geometry is neither square planar nor tetrahedral but something in between such as trigonal bipyramidal with a missing equatorial ligand (seesaw). Recent computational studies have suggested that the triplet spin state (high-spin) is more accurate based on the Ni geometry.[9] In addition, a previous study by Wu and Hall examined these questions and others and came to the conclusion that two-state reactivity could play an important role in the mechanism of [NiFe] hydrogenase, a suggestion previously not considered, and that with this two-state model H_2 can bind to both the Ni and Fe centers.[11] Binding at Fe is preferred if Ni is high-spin, but binding at Ni is preferred if it is low-spin. In a followup to

*To whom correspondence should be addressed. E-mail: hall@science.tamu.edu.

(1) Albract, S. P. J. *Biochim. Biophys. Acta* **1994**, *167*, 1188.
(2) For NiFeSe, see: Garcin, E.; Vernede, X.; Hatchikian, E. C.; Volbeda, A.; Frey, M.; Fontecilla-Camps, J. C. *Structure* **1999**, *7*, 557.
(3) Adams, M. W. W. *Biochim. Biophys. Acta* **1990**, *115*, 1020.
(4) Thauer, R. K.; Klein, A. R.; Harmann, G. C. *Chem. Rev.* **1996**, *96*, 3031.
(5) (a) Higuchi, Y.; Ogata, H.; Miki, K.; Yasuoka, N.; Yagi, T. *Structure* **1999**, *7*, 549. (b) Volbeda, A.; Charon, M. H.; Piras, C.; Hatchikian, E. C.; Frey, M.; Fontecilla-Camps, J. C. *Nature* **1995**, *373*, 580. (c) Volbeda, A.; Garcin, E.; Piras, C.; de Lacey, A. L.; Fernandez, V. M.; Hatchikian, E. C.; Frey, M.; Fontecilla-Camps, J. C. *J. Am. Chem. Soc.* **1996**, *118*, 12989. (d) Volbeda, A.; Martin, L.; Cavazza, C.; Matho, M.; Faber, B. W.; Roseboom, W.; Albract, S. P. J.; Garcin, E.; Fousset, M.; Fontecilla-Camps, J. C. *J. Biol. Inorg. Chem.* **2005**, *10*, 239. (e) Ogata, H.; Hirota, S.; Nakahara, A.; Komori, H.; Shibata, N.; Kato, T.; Kano, K.; Higuchi, Y. *Structure* **2005**, *13*, 1635.
(6) Siegbahn, P. E. M.; Tye, J. W.; Hall, M. B. *Chem. Rev.* **2007**, *107*, 4414.
(7) (a) Kowal, A. T.; Zambrano, I. C.; Moura, I.; Moura, J. J. G.; LeGall, J.; Johnson, M. K. *Inorg. Chem.* **1988**, *27*, 1162. (b) Wang, C. P.; Franco, R.; Moura, J. J. G.; Moura, I.; Day, E. P. *J. Biol. Chem.* **1992**, *267*, 7378.
(8) Wang, H.Ralston, C. Y.; Patil, D. S.; Jones, R. M.; Gu, W.; Verhagen, M.; Adams, M.; Ge, P.; Riordan, C.; Marganian, C. A.; Mascharak, P.; Kovacs, J.; Miller, C. G.; Collins, T. J.; Brooker, S.; Croucher, P. D.; Wang, K.; Stiefel, E. I.; Cramer, S. P. *J. Am. Chem. Soc.* **2000**, *122*, 10544.
(9) (a) Niu, S.; Thomson, L. M.; Hall, M. B. *J. Am. Chem. Soc.* **1999**, *121*, 4000. (b) Fan, H.-J.; Hall, M. B. *J. Biol. Inorg. Chem.* **2001**, *6*, 467. (c) Li, S.; Hall, M. B. *Inorg. Chem.* **2001**, *40*, 18. (d) Niu, S.; Hall, M. B. *Inorg. Chem.* **2001**, *40*, 6201. (e) Fan, H.-J.; Hall, M. B. *J. Am. Chem. Soc.* **2002**, *124*, 394. (f) Pardo, A.; De Lacey, A. L.; Fernández, V. M.; Fan, H.-J.; Fan, Y.; Hall, M. B. *J. Biol. Inorg. Chem.* **2006**, *11*, 286. (g) Pardo, A.; De Lacey, A. L.; Fernández, V. M.; Fan, Y.; Hall, M. B. *J. Biol. Inorg. Chem.* **2007**, *12*, 751.
(10) Most favorable protonation site, S(H), determined from ref 12.
(11) Wu, H.; Hall, M. B. *C. R. Chim.* **2008**, *11*, 790.

 Published on Web 06/17/2010

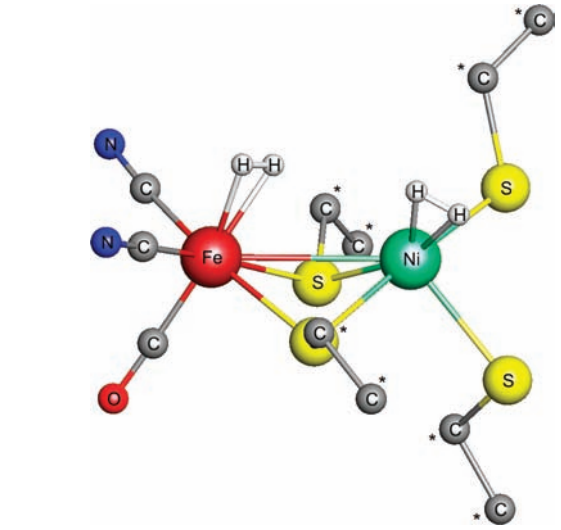

Figure 1. DFT-optimized structure of the active site of [NiFe] hydrogenase from *D. gigas*[6] shown with molecular H_2 bound to both the Ni and Fe binding sites. Frozen C atoms are denoted with asterisks.

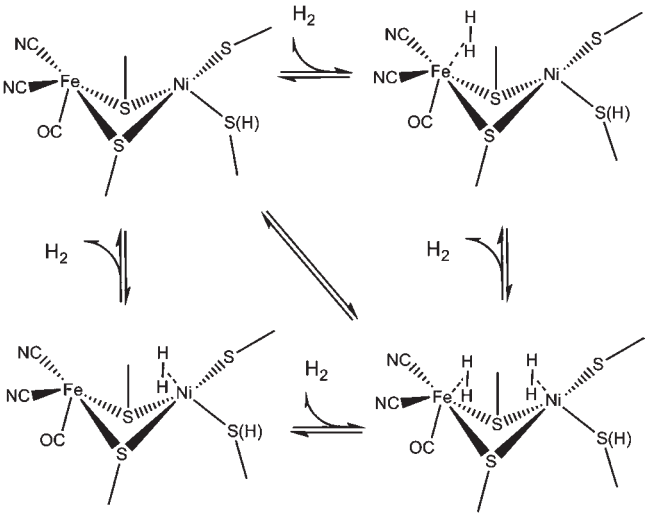

Figure 2. H_2 binding modes to the Ni−SI form of [NiFe] hydrogenase: **1** Ni−SI with no H_2; **2** H_2 bound to Fe; **3** H_2 bound to Ni; **4** H_2 bound to Ni and Fe. S(H) may be unprotonated, S, or protonated, SH.[10]

these results, we have examined the various modes of H_2 binding and have discovered a potential hydrogen bottleneck that exists because H_2 can bind to both the Ni and Fe simultaneously, **4**, possibly slowing further activity. This suggestion relies on the idea that both metal centers are vital to enzyme activity. We believe this to be true, although further mechanistic work is required to connect this potential bottleneck with actual catalyst inhibition. Herein, we detail the results of a density functional theory (DFT) study with the focus of examining various H_2 binding modes with both the singlet and triplet active sites in protonated and unprotonated forms.[10]

The initial calculations were performed with the hybrid functional B3LYP[12] using *Gaussian 03*.[13] This functional is known to produce good descriptions of reactions for transition-metal-containing compounds.[14] S, Ni, and Fe were described using the LANL2DZ[15] pseudo potential and basis set with modified 4p orbitals on Ni and Fe[16] and S atoms augmented with d orbitals.[17] All other atoms were modeled using the 6-31G(d′,p′) basis set.[18] Additionally, each species was examined with TPSS[19] for comparison. While numbers from two different functionals seem to complicate the issue, it is thought that B3LYP favors high-spin (HS) states while TPSS favors low-spin (LS) states. The active site geometries were restricted as shown in Figure 1.

Table 1. Relative Electronic Energies in kcal/mol for Species **1**−**4** (with Respect to $\mathbf{1_{HS}}$ for Each Row, p = protonated)

functional	$\mathbf{1_{LS}}$	$\mathbf{1_{HS}}$	$\mathbf{2_{LS}}$	$\mathbf{2_{HS}}$	$\mathbf{3_{LS}}$	$\mathbf{3_{HS}}$	$\mathbf{4_{LS}}$	$\mathbf{4_{HS}}$
B3LYP	10.0	0.0	9.2	−2.7	10.9	NA	NA	NA
TPSS	1.4	0.0	NA	−3.6	−4.7	NA	4.0	NA
	$\mathbf{1_{LSp}}$	$\mathbf{1_{HSp}}$	$\mathbf{2_{LSp}}$	$\mathbf{2_{HSp}}$	$\mathbf{3_{LSp}}$	$\mathbf{3_{HSp}}$	$\mathbf{4_{LSp}}$	$\mathbf{4_{HSp}}$
B3LYP	7.4	0.0	7.1	−3.4	5.6	NA	7.9	NA
TPSS	−3.8	0.0	−0.4	−6.1	−8.8	NA	−2.7	NA

When deprotonated, the high-spin ground-state species, $\mathbf{1_{HS}}$, is favored (Table 1). While TPSS calculations were consistent with B3LYP in the designation of a high-spin ground state, they showed a significant decrease in the energy difference between the two spin states. In the B3LYP structures, the Fe environments of the high- and low-spin state species are similar, with the only difference arising from the decrease in the Ni−Fe distance from 3.20 Å in $\mathbf{1_{HS}}$ to 3.03 Å in $\mathbf{1_{LS}}$. Predictably, the Ni environments have changed more substantially, with a slight shortening of all four Ni−S distances when going from high to low spin. According to Mulliken spin densities, the two unpaired spins in $\mathbf{1_{HS}}$ reside primarily on the Ni atoms (1.41 electrons) and the four S atoms (0.56 electrons). The overall geometries of the TPSS complexes have not changed considerably, and the only notable difference is a shortening of the Ni−Fe distance by about 0.25 Å for both the high- and low-spin species.

Upon protonation, the low-spin species is stabilized relative to the high-spin species (Table 1). The B3LYP geometries show an increase in the Ni−S(H) distance of about 0.1 Å and a corresponding decrease in the trans Ni−S due to protonation. The unpaired spins in the triplet species still reside primarily on the Ni atoms (1.40 electrons) and on the surrounding S atoms (0.59 electrons total). The larger degree of stabilization of the low-spin species shown with the TPSS functional reversed the order of the two spin states, resulting in a low-spin ground state for this functional. We believe a significant contributor to this discrepancy is the significant geometric change in which the Ni in species $\mathbf{1_{LSp}}$**(TPSS)** interacts with one of the two CN ligands, which is now in a semibridging position (Ni−CN 2.53 Å).

H_2 binding at the Fe center was examined for both the protonated and unprotonated forms of the active site for high

(12) (a) Becke, A. D. *J. Chem. Phys.* **1993**, *98*, 5648. (b) Lee, C.; Yang, W.; Parr, R. G. *Phys. Rev. B* **1988**, *37*, 785.
(13) Frisch, M. J. et al. *Gaussian 03*, revision E.01; Gaussian, Inc.: Pittsburgh, PA, **2003**.
(14) Niu, S.; Hall, M. B. *Chem. Rev.* **2000**, *100*, 353.
(15) (a) Wadt, W. R.; Hay, P. J. *J. Chem. Phys.* **1985**, *82*, 284. (b) Hay, P. J.; Wadt, W. R. *J. Chem. Phys.* **1985**, *82*, 299.
(16) Couty, M.; Hall, M. B. *J. Comput. Chem.* **1996**, *17*, 1359.
(17) Höllwarth, A.; Böhme, M.; Dapprich, S.; Ehlers, A. W.; Gobbi, A.; Jonas, V.; Köhler, K. F.; Stegmann, R.; Veldkamp, A.; Frenking, G. *Chem. Phys. Lett.* **1993**, *208*, 237.
(18) (a) Hariharan, P. C.; Pople, J. A. *Chem. Phys. Lett.* **1972**, *16*, 217. (b) Francl, M. M.; Pietro, W. J.; Hehre, W. J.; Binkley, J. S.; Gordon, M. S.; DeFrees, D. J.; Pople, J. A. *J. Chem. Phys.* **1982**, *77*, 3654.
(19) Tao, J. M.; Perdew, J. P.; Staroverov, V. N.; Scuseria, G. E. *Phys. Rev. Lett.* **2003**, *91*, 146401.

and low spin (species **2**). Like the active site without H_2, the high-spin species $\mathbf{2_{HS}}$ is favored considerably when unprotonated. In fact, binding of H_2 to the Fe center in the unprotonated low-spin case was not located at all with TPSS because all attempts to locate species $\mathbf{2_{LS}}$(**TPSS**) resulted in H_2 transferring to the Ni center. In addition, H_2 binding is favorable for all cases. The Fe environments of the high- and low-spin state species are similar, apart from a decrease in the Ni−Fe distance for the low-spin case. The H−H distance has increased slightly to ∼0.80 Å for all three cases, indicating that the H−H bond is still intact.[20] The Fe−H interaction is slightly asymmetric. Other than increased Ni−Fe distances, the Ni centers demonstrate almost no change from the corresponding hydrogen-free cases. Upon protonation, the low-spin species are slightly stabilized relative to the high-spin species. The new geometries do not significantly vary from the corresponding hydrogen-free cases and will not be discussed further.

Compared to Fe, H_2 binding at the Ni center was more erratic because the binding modes seem to be influenced more strongly by the protonation state and spin multiplicity. In fact, no Ni−H_2 binding modes were located for the high-spin species at all, regardless of protonation, because all attempts with both functionals either simply ejected H_2 or transferred it to the Fe center. The Fe environment remains similar to that of $\mathbf{1_{HS}}$, again with a decrease in the Ni−Fe distance. The Ni complexation now resembles a trigonal-bipyramidal geometry with two S atoms and η^2-H_2 as the three equatorial ligands. H_2 binding is slightly uphill compared to the unbound singlet case for B3LYP, while TPSS calculations predict binding on the Ni site to be favorable compared to the unbound ground state. Again, the H_2 distances have only increased slightly to ∼0.80 Å, indicating little change from free H_2. Like with Fe, the Ni−H_2 interaction is slightly asymmetric. Notably, one of the bridging Ni−S distances has increased to 2.50 Å, while all other Ni−S distances are ∼2.30 Å. Once again, TPSS shows a decrease in the Ni−Fe distance to 2.68 Å as well as increased hydrogen activation with a slightly longer H−H distance and shorter Ni−H distances, demonstrating more hydrogen activation in $\mathbf{3_{HS}}$ than in any of the preceding species.

Upon protonation, H_2 binding to the Ni center improves with B3LYP, making its energy downhill compared to the unbound singlet case. Again, the TPSS functional shows binding on the Ni site favorable with a $\Delta E = -8.8$ kcal/mol compared to the unbound ground state. The geometries have changed little upon protonation, with the only significant change being an increase in the Ni−S(H) bond and the corresponding shortening of the trans Ni−S and Ni−Fe bonds. Hydrogen activation is still minimal with an H−H distance of ∼0.80 Å. TPSS structures show decreases in the Ni−Fe and Ni−H distances and an increased H−H bond.

In agreement with previous results, these data demonstrate the possibility of H_2 binding to both the Ni and Fe centers, with the preferred binding mode modulated by the spin multiplicity on the Ni center (two-state reactivity) as well as the protonation state of adjacent cysteine ligands. Two questions have been previously ignored. Because there are multiple binding sites for H_2 (e.g., both Fe and Ni), is there then the possibility of simultaneously binding two H_2 molecules and, if so, what potential impact would this have on the overall process? On the basis of our calculations, we find the answer to the former to be "yes". An intermediate has been located with H_2 bound to both the Ni and Fe. Only the low-spin version of this intermediate, $\mathbf{4_{LS}}$, is stable for both functionals (for B3LYP, only the protonated low-spin version, $\mathbf{4_{LSp}}$, is stable). This is understandable based on the results above that binding to the Ni (species **3**) only happened for low-spin cases and that these binding modes were stabilized upon protonation. All other attempts to locate this species (e.g., $\mathbf{4_{LS}}$(**B3LYP**) or $\mathbf{4_{HSp}}$) resulted in a loss of one of the two H_2 molecules and conversion to one of the previously discussed species. Species $\mathbf{4_{LSp}}$ is slightly uphill compared to the unbound singlet case (0.5 kcal/mol), putting it 7.9 kcal/mol above the unbound ground state for B3LYP. Calculations with the TPSS functional once again show Ni with an increased affinity toward molecular H_2, and stable species with two molecules of H_2 bound (one on Ni and one on Fe) were located for both the unprotonated and protonated low-spin species with $\Delta E = 4.0$ and -2.7 kcal/mol. While this demonstrates that two H_2 molecules can simultaneously bind, it is still unclear what the impact is. Potentially, this could lead to a hydrogen bottleneck and subsequent enzyme inhibition if both metals are involved in the hydrogen oxidation as we believe they are.

Here, modern DFT on a simplified active site model provides further evidence that both the high- and low-spin species of the Ni−SI forms may play an important role in the reactivity of this enzyme with molecular H_2. In addition to examining H_2 binding modes to both the Ni and Fe of the active site, we have also suggested the possibility that the active site of this enzyme could bind two molecules of H_2 simultaneously at both metal centers and in effect create a potential hydrogen bottleneck in which very high concentrations could lead to a decrease in the rate of hydrogen oxidation. Interestingly, the two binding sites and the two spin states lead one to wonder about the possibility of two or more reaction mechanisms. Historically, we have favored oxidation to Ni^{III} prior to hydrogen activation because oxidation lowers the barrier to cleavage and stabilizes the resulting five-coordinate Ni.[8] Recently, it has been suggested that the Ni could instead be reduced to Ni^{I}, which would then cleave H_2 homolytically by oxidative addition.[21] The predicted bottleneck caused by the coordination of two H_2 molecules could be relieved by this latter route. Thus, the enzyme may have multiple reaction paths available whose use depends on conditions such as the H_2 concentration and electron availability. Further mechanistic work by our group and others is needed to answer this for sure.

Acknowledgment. The authors thank the National Science Foundation (Grants CHE-0518074, CHE-0541587, and CHE-0910552) and The Welch Foundation (Grant A-0648) for financial support. Professor Fraser Armstrong (Oxford) is acknowledged for suggesting this study.

Supporting Information Available: Additional structures, Cartesian coordinates, and energies for all species. This material is available free of charge via the Internet at http://pubs.acs.org.

(20) The H2 bond was calculated to be ∼0.75 Å for both functionals.

(21) Lill, S. O. N.; Siebahn, P. E. M. *Biochemistry* **2009**, *48*, 1056.